Parametric Optimization of Nd:YAG Laser Microgrooving of Alumina Ceramic Using Integrated RSM-PSO Approach

Anil Swain, Santosh Kumar Sahu, Anisha Ekka and Sudhansu Ranjan Das

Abstract In order to manufacture various products with well-suited quality by machining, appropriate choice of process parameters is of prime importance. Hence, the present work focuses on modeling and optimization during Nd:YAG laser microgrooving of K-60 alumina ceramic material with an objective to find the optimum process parameters settings for minimizing the upper width deviation. The experiments are performed as per Box–Behnken design of experiments (BBDOEs) with four process parameters (diode current, pulse frequency, scanning speed, and number of passes) for parametric optimization in order to control the technological response characteristic (upper width deviation) of the precision microgrooves on K-60 alumina. Analysis of variance (ANOVA), response surface methodology (RSM), and particle swarm optimization (PSO) are subsequently proposed for predictive modeling and process optimization. Result shows the optimal setting of machining variables in laser microgrooving of K-60 alumina ceramic at pulse frequency of 4.4 kHz, diode current of 17 amp, scan speed of 35 mm/s, number of passes as 12, with estimated groove upper width deviation of 0.02669 μm. The methodology described here is expected to be highly beneficial for manufacturing industries.

Keywords Laser microgrooving · K-60 alumina ceramic · ANOVA · RSM · PSO

1 Introduction

The recent technology has been advancing to infinite extent in search of newer materials and alloys with high hardness, strength, and less weight which are very difficult to be machined with the conventional machining processes for achieving

A. Swain · A. Ekka · S. R. Das (✉)
Department of Production Engineering, VSSUniversity of Technology, Burla 768018, India
e-mail: das.sudhansu83@gmail.com

S. K. Sahu
Department of Mechanical Engineering, VSS University of Technology, Burla 768018, India

the required accuracy and precision. Nowadays, there is a vast demand for the well-finished products of alumina ceramic materials with high accuracy and complex integrated designs. Such features on a component can be achieved only through the advanced manufacturing process, especially by laser beam machining. In case of micromachining, the feature size is less than 1 mm. Hence, lasers are increasingly employed for a precise micromachining because their beams can be focused accurately on microscopic areas, and attributed to a number of advantages which are normally applicable to whole range of the materials processing applications, like, non-contact processing, high productivity, eradication of the finishing operations, minimized cost of processing, and enhanced the quality of product, maximise material utilization, green manufacturing and minimize the heat affected zone [1]. The above-cited advantages can only be obtained with appropriate selection of process parameters. Researchers have employed various methods: multiple regression analysis (MRA) [2, 3] and artificial neural network (ANN) [4–6] for mathematical modeling in order to predict the responses and Taguchi method [7–9], response surface method(RSM) [10–12], genetic algorithm (GA) [13–15], particle swarm optimization (PSO) [16, 17] for optimization the controlled process parameters during laser micromachining process that have been explored as productivity and reliable tool in advanced computing technology for high-quality frameworks since it gives a straightforward, skilled, and systematically optimize the output, such as cost, quality, and performance. The proper utilization along with appropriate adjustment of machining controllable process parameters is of main importance for achieving fine grade of microgrooves, which generally utilize proper time and effort due to the frequently changing behavior of the laser micromachining process. Thus, the present study focuses on development of mathematical model and response parametric optimization during laser microgrooving of alumina ceramic using statistical approach such as RSM followed by computational approach like PSO.

2 Experimental Procedure

A 75-W diode-pumped Nd:YAG laser (make: Sahajanand, model: SPRIGO LD) was used to conduct the experiments which has assist gas supply unit. During experiment, the laser beam (focal length of 77 mm) has been set at surface of the workpiece as the focal plane which resulted in laser beam spot size around 21 μm. In the present research, K-60 alumina ceramic plate of dimension (25 mm * 25 mm * 4 mm) is considered as the workpiece material for experimentation, subjected to microgrooving by multiple laser pulses (DPSS Nd:YAG laser treatment) with actual peak power vary between 0.7 and 5 kW. In the current investigation diode current, pulse frequency, scan speed, and number of pass are considered as the input process parameters which influence the technological performance of laser microgrooving such as upper width deviation. The different process parameters and their values are shown in Table 1.

Using the above-mentioned process parameters (4) each with four different levels, a well-designed experimental layout is formulated in conformance with

Table 1 Process parameters and levels

Control parameters	Symbols	Units	Levels				
			-2	-1	0	1	2
Diode current	I	amp	17	19	21	23	25
Pulse frequency	F	kHz	2.8	3.2	3.6	4.0	4.4
Scan speed	S	mm/s	35	45	55	65	75
Number of passes	N		8	9	10	11	12

Box–Behnken design of experiments (BBDOEs) which is consisting of thirty one (31) number of trials. Design of experimental plan with actual value of process parameters and measured response is presented in Table 2. The upper width deviation (UWD) of machined microgroove is measured by utilizing optical microscope (model: STM6, make: Olympus). The schematic view of experimental work and methodology proposed in the current study is presented in Fig. 1.

For parametric optimization, particle swarm optimization (PSO) approach has been employed, which is a biographically inspired stochastic population-based computational approach, which simulates the collective social–psychological behavior of animals such as fish schooling, bird flocking in order to provide the sufficiently good solution to a complex optimization problem. It is a search algorithm for minimizing the functions where each member of the population is called swarm. This method is much powerful and very popular because of its simplicity of execution as well as ability to briskly converge to good solution. Every particle is considered as a point in N-dimensional space that modifies its "flying" to its own flying experience as well as experience of flying other particles. A PSO system integrates local search methods with global search methods aiming to stabilize exploitation and exploration. PSO algorithm maintains multiple potential solutions at one time. The basic computational principle includes evaluating the present position of the particle, comparing it with personal best as well as global best and imitate self and others. The position of every particle in the swarm is influenced both by best optimist position through its own movement and surroundings. During each iteration of the algorithm, each solution is evaluated by an objective function to determine its fitness. All the particles are initiated randomly and evaluated by finding the p_{best} (best value of each particle) and g_{best} (best value in the entire swarm). In basic PSO method, the velocity of particle is evaluated mathematically by:

$$v_i^{k+1} = w v_i^k + C_1 R_1 \left(p_{\text{best}_i} - x_i^k \right) + C_2 R_2 \left(g_{\text{best}} - x_i^k \right) \tag{1}$$

Mathematically, the update position of every particle can be described by using the following equation:

$$x_i^{k+1} = x_i^k + v_i^{k+1} \tag{2}$$

where v_i^k and x_i^k are the ith particle's velocity and update position at iteration kth w.r.t. search space; R_1 and R_2 are two random numbers fall in between 0 and 1; C_1

Table 2 Design of experimental plan associated with results

Run	Coded values				Actual settings				Response
	I	F	S	N	Diode current (amp)	Pulse frequency (kHz)	Scan speed (mm/s)	No. of passes	UWD (μm)
1	1	1	−1	−1	23	4.0	45	9	0.07017
2	0	0	0	−2	21	3.6	55	8	0.037225
3	−1	−1	1	1	19	3.2	65	11	0.039325
4	−1	1	−1	−1	19	4.0	45	9	0.032250
5	0	0	0	0	21	3.6	55	10	0.053233
6	0	0	0	2	21	3.6	55	12	0.066
7	0	0	0	0	21	2.8	55	10	0.05315
8	−1	1	1	−1	19	4.0	65	9	0.027662
9	−1	0	1	1	19	3.6	65	11	0.02373
10	−1	−1	−1	−1	19	3.2	45	9	0.021243
11	0	0	0	0	21	3.6	55	10	0.029759
12	0	0	0	0	21	3.6	55	10	0.028759
13	2	0	0	0	25	3.6	55	10	0.110604
14	−1	−1	1	−1	19	3.2	65	9	0.036215
15	1	−1	−1	−1	23	3.2	45	9	0.063806
16	1	−1	−1	1	23	3.2	45	11	0.072296
17	0	0	0	0	21	3.6	55	10	0.053152
18	1	−1	1	−1	23	3.2	65	9	0.06485
19	0	0	2	0	21	3.6	75	10	0.036153
20	−1	1	−1	1	19	4.0	45	11	0.031877

(continued)

Table 2 (continued)

| Run	Coded values				Actual settings				Response
	I	F	S	N	Diode current (amp)	Pulse frequency (kHz)	Scan speed (mm/s)	No. of passes	UWD (µm)
21	0	0	0	0	21	3.6	55	10	0.038259
22	−1	−1	−1	1	19	3.2	45	11	0.017
23	0	0	0	0	21	3.6	55	10	0.040386
24	0	0	−2	0	21	3.6	35	10	0.046825
25	−1	1	−1	−1	19	4.0	45	11	0.032880
26	1	−1	1	−1	23	3.2	65	11	0.066986
27	0	2	0	0	21	4.4	55	10	0.024494
28	1	1	1	1	23	4.0	65	11	0.074431
29	0	0	0	0	21	3.6	55	10	0.005296
30	1	1	1	−1	23	4.0	65	9	0.057
31	−1	0	0	0	17	3.6	55	10	0.002151
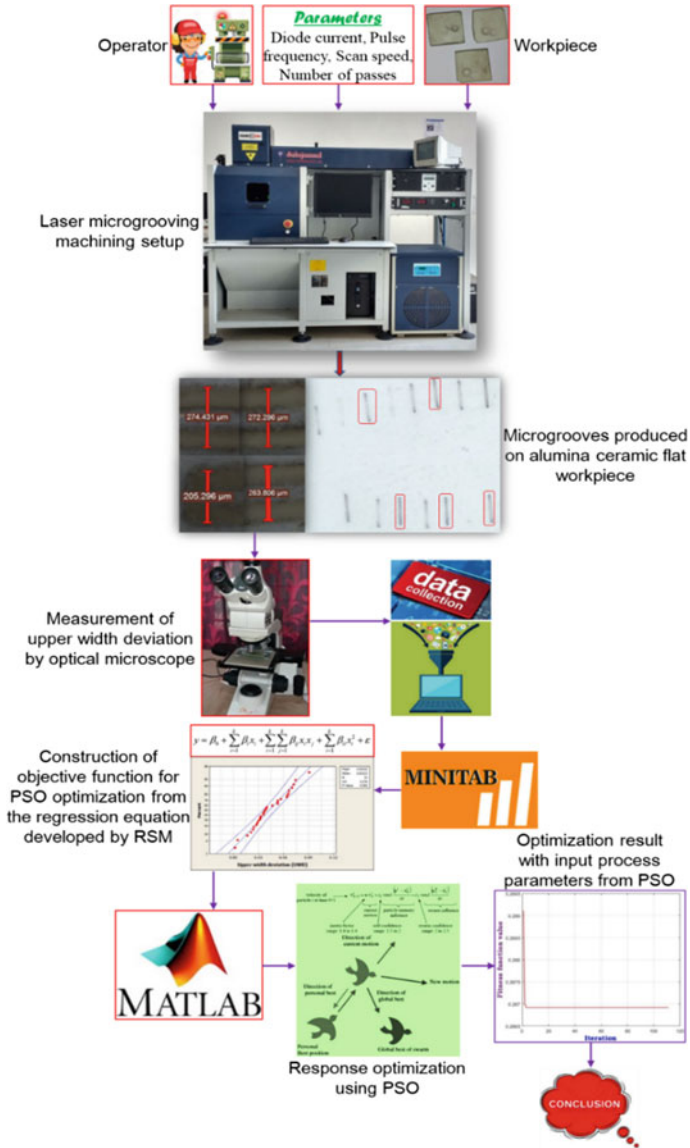
Fig. 1 Schematic of methodology and experimental setup proposed

and C_2 are the acceleration coefficients correspond to p_{best} and g_{best}, respectively; and w is the inertia weight can be assessed by the following equation:

$$w = w_{max} - \left[\frac{w_{max} - w_{min}}{\text{iter}_{total}} \times \text{iter}_{current} \right] \tag{3}$$

3 Results and Discussion

3.1 Development of Predictive Model

The results of response characteristic, i.e., upper width deviation (UWD) which were obtained in accordance of BBDOEs, were analyzed in Minitab16 through response surface methodology (RSM), developed the mathematical model to find out the best fit of correlation between the upper width deviation of the microgrooved component with the input parameters such as diode current (I), pulse frequency (F), scanning speed (S), and number of passes (N). Regression equation in the second order (i.e., quadratic model) for the response UWD is presented by:

$$
\begin{aligned}
UWD &= 0.874829 - 0.045604 * I - 0.090648 * F + 0.007902 * S \\
&\quad - 0.109260 * N + 0.001069 * I^2 + 0.009591 * F^2 + 0.00000 * S^2 \\
&\quad + 0.003086 * N^2 + 0.001689 * IF - 0.000200 * IS + 0.001723 * IN \\
&\quad - 0.0011363 * FS + 0.004777 * FN - 0.000033 * SNR^2 \\
&= 91.11\%, R^2(\text{adj.}) = 83.34\%
\end{aligned}
\tag{4}
$$

To avoid the misleading conclusion, statistical analysis is performed for the proposed RSM model (UWD) by employing ANOVA in order to check its adequacy and validity, as shown in Table 3. The estimate F-value of the model for UWD is 11.72, which shows the excellent significance of model because of lower magnitude of F-table value (2.46) at 95% of confidence level. Moreover, the suggested quadratic model is noticed statistically significant as the P-value is under 0.05. Particularly, the model explains the R^2 value (i.e., coefficient of determination) of 0.91 which is very close to unity (1) ensuring the excellent fit for the model with better predictive ability. Finally, normal probability plot combined with Anderson–Darling test for UWD is illustrated in Fig. 2 and confirms the residuals are distributed nearly close to a straight line revealing that the errors are dispersed normally and specifying that the terms corresponding to the model are significant. With P-value (0.392 for UWD) received from Anderson–Darling test is greater than significance level value (0.05), which confirms the adequacy of model as no reason was observed for the rejection of null hypothesis. Hence, the proposed predictive model can be utilized as objective function for particle swarm optimization.

Table 3 Results of ANOVA for response model, UWD

| Source	DF	Seq. SS	Adj. SS	Adj. MS	F	P	Remark
Regression	14	0.012878	0.012878	0.000920	11.72	0.000	Significant
Linear	4	0.011633	0.000709	0.000177	2.26	0.108	
Square	4	0.000629	0.000739	0.000185	2.35	0.098	
Interaction	6	0.000553	0.000553	0.000092	1.17	0.368	
Residual error	16	0.001256	0.001256	0.000079			
Lack of fit	10	0.000658	0.000658	0.000066	0.66	0.733	
Pure error	6	0.000598	0.000598	0.000100			
Total	30	0.014135					
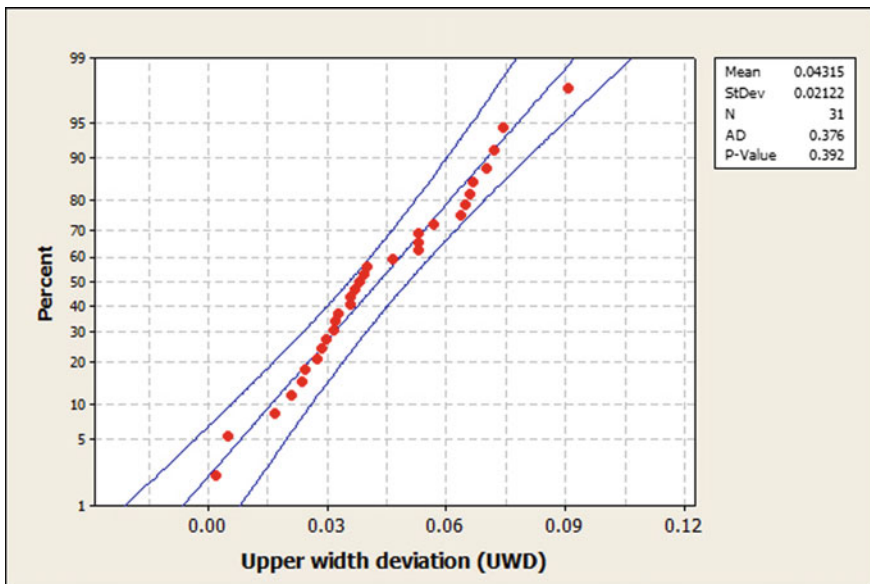
Fig. 2 Normal probability plot for UWD

3.2 Response Optimization Using PSO

The predictive mathematical model for upper width deviation developed by RSM, shown in Eq. (4), is considered as an objective function for particle swarm optimization. Figure 3 presents the convergence plot, which aims to minimize the above-mentioned response in the existence of PSO algorithm-specific parameters. In this work, the critical parameters are considered about the population size of 120, acceleration factors (C_1 and C_2) of 1.2, maximum number of iterations equal to 200, minimum and maximum values of inertia weights of 0.35 and 0.5, respectively. By

Fig. 3 Convergence curve for PSO algorithm
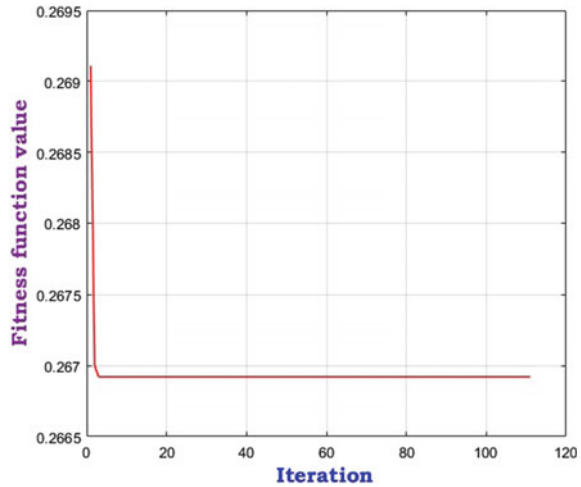
using PSO, the optimal microgrooving settings in laser machining of K-60 alumina ceramic are diode current 17 amp, pulse frequency 4.4 kHz, scan speed 35 mm/s, number of passes as 12, with estimated groove upper width deviation (UWD) of 0.02669 µm.

4 Conclusion

Empirical models proposed for the technological response characteristic such as upper width deviation have R-Square value close to one and P-value less than 0.05, which ensured the greater statistical significance with the excellence of fit for the model. The normal probability plot ensures that the residuals distributed fairly near to a straight line showing the normality dispersion of errors as well as implying the sources associated with the model are significant. Anderson–Darling test for model shows adequate, as P-value is over 0.05 at 95% confidence level. Response optimization employing PSO technique shows the optimal setting of machining variables in laser microgrooving of K-60 alumina ceramic at pulse frequency of 4.4 kHz, diode current of 17 amp, scan speed of 35 mm/s, number of passes as 12, with estimated groove upper width deviation of 0.02669 µm. The suggested multiple approaches (experimental, statistical, and computational) are reliable methodologies for improving laser microgrooving process and can be used in model predictive control, real-time process monitoring, and optimization in different machining processes.

References

1. Darwish SMH, Ahmed N, Al-Ahmari AM (2017) Laser beam micro-milling of micro-channels in aerospace alloys. Springer Nature Singapore, pp 15–80. https://doi.org/10.1007/978-981-10-3602-6 (2017)
2. Dhupal D, Doloi B, Bhattacharyya B (2009) Modeling and optimization on Nd:YAG laser turned micro-grooving of cylindrical ceramic material. Opt Lasers Eng 47:917–925
3. Kibria G, Doloi B, Bhattacharyya B (2013) Predictive model and process parameters optimization of Nd:YAG laser micro-turning of ceramics. Int J Adv Manuf Technol 65:213–229
4. Biswas R, Kuar AS, Biswas SK, Mitra S (2010) Artificial neural network modelling of Nd:YAG laser microdrilling on titanium nitride—alumina composite. J Eng Manuf 224:473–482
5. Kibria G, Doloi B, Bhattacharyya B (2014) Modelling and optimization of Nd: YAG laser micro-turning process during machining of aluminum oxide (Al_2O_3) ceramics using response surface methodology and artificial neural network. Manuf Rev 1:1–8
6. Dixit SR, Das SR, Dhupal D (2018) Parametric optimization of Nd:YAG laser microgrooving on aluminum oxide using integrated RSM-ANN-GA approach. J Ind Eng Int https://doi.org/10.1007/s40092-018-0295-1 (2018)
7. Kuar AS, Acherjee B, Ganguly D, Mitra S (2012) Optimization of Nd:YAG Laser parameters for microdrilling of alumina with multiquality characteristics via grey-Taguchi method. Mater Manuf Processes 27:329–336
8. Mohammed M, Umer U, Rehman A, Al-Ahmari A, El-Tamimi A (2018) Microchannels fabrication in alumina ceramic using direct Nd:YAG laser writing. Micromachines 9:371
9. Yang K, Xia Y, Li L, He N, Zhang Y, Zhang T, Wang Y (2018) Experimental study on hybrid machining of laser irradiation and grinding for sharpening of a CVD diamond micro-milling tool. Int J Adv Manuf Technol. https://doi.org/10.1007/s00170-018-1624-7 (2018)
10. Kibria G, Doloi B, Bhattacharyya B (2012) Optimisation of Nd: YAG laser micro-turning process using response surface methodology. Int. J. Precis Technol 3:14–36
11. Biswas R, Kuar AS, Mitra S (2015) Process optimization in Nd:YAG laser microdrilling of alumina–aluminium interpenetrating phase composite. J Mater Res Technol 4:323–332
12. Kibria G, Doloi B, Bhattacharyya B (2013) Investigation and analysis on pulsed Nd:YAG laser micro-turning process of aluminium oxide (Al_2O_3) ceramic at various laser defocusing conditions. Int. J Adv Manuf Technol 76:17–27
13. Nandi S, Kuar AS (2015) Parametric optimisation of Nd:YAG laser micro-drilling of alumina using NSGA II. Int. J Mach Machinability Mater 17:1–21
14. Mohammed MK, Umer U, Al-Ahmari A (2017) Optimization of laser micro milling of alumina ceramic using radial basis functions and MOGA-II. Int J Adv Manuf Technol 91:2017–2029
15. Abdo BMA, El-Tamimi AM, Anwar S, Umer U, Alahmari AM, Ghaleb MA (2018) Experimental investigation and multi-objective optimization of Nd:YAG laser micro-channeling process of zirconia dental ceramic. Int J Adv Manuf Technol 98(5–8):2213–2230
16. Kalita K, Shivakoti I, Ghadai RK (2017) Optimizing process parameters for laser beam micro-marking using genetic algorithm and particle swarm optimization. Mater Manuf Processes 32:1101–1108
17. Dhupal D, Mohanty S, Dixit SR, Das SR, Nanda BK (2018) Micromachining on Al-SiC based metal matrix composite using DPSS laser. Mater Today Proc 5:11304–11318